Localized structures in a nonlinear wave equation stabilized by negative global feedback: one-dimensional and quasi-two-dimensional kinks

Horacio G. Rotstein*

Department of Mathematics and Center for Biodynamics, Boston University, Boston, MA, 02215

Anatol A. Zhabotinsky† and Irving R. Epstein‡

Department of Chemistry and Volen Center for Complex Systems, Brandeis University, Waltham, MA, 02454

(Dated: January 26, 2006)

Abstract

We study the evolution of fronts in a nonlinear wave equation with global feedback. This equation generalizes the Klein-Gordon and sine-Gordon equations. Extending previous work, we describe the derivation of an equation governing the front motion, which is strongly nonlinear, and, for the two-dimensional case, generalizes the damped Born-Infeld equation. We study the motion of one- and two-dimensional fronts, finding a much richer dynamics than for the classical case (with no global feedback), leading in most cases to a localized solution; i.e., the stabilization of one phase inside the other. The nature of the localized solution depends on the strength of the global feedback as well as on other parameters of the model.

*Electronic address: horacio@math.bu.edu

†Electronic address: zhabotin@brandeis.edu

‡Electronic address: epstein@brandeis.edu

I. INTRODUCTION

In this paper we study the existence of localized one-dimensional fronts and two-dimensional front-like structures in the following nonlinear wave equation with global coupling for the order parameter ϕ:

$$\phi_{tt} + \eta\ \phi_t = D\ \Delta\phi + \alpha\ [\ f(\phi) + h\ ] + \gamma\ <\ g(\phi)\ >, \tag{1}$$

defined on a bounded domain Ω in $\mathbf{R}$ or $\mathbf{R^2}$. In (1) η, D and γ are the dissipation (damping), diffusion (local coupling) and global coupling parameters respectively. The function f is bistable (the derivative of a double well potential function having two equal minima); i.e., a real odd function vanishing at three points in the closed interval $[a_-, a_+]$ located at a_-, a_0 and a_+ with $f'(a_\pm) < 0$ and $f'(a_0) > 0$. The constant h, assumed to be small in absolute value, specifies the difference of the potential minima of the system; i.e., $f(\phi) + h$ is the derivative of a double well potential function with one local minimum and one global minimum. The parameter α is proportional to the height of the barrier of the double well potential or to the slope of $f(\phi)$ at its unstable fixed point. The prototype examples for $h = \gamma = 0$ are the damped Klein-Gordon and sine-Gordon equations where $f(\phi) = (\phi - \phi^3)/2$ ($a_\pm = \pm 1$) and $f(\phi) = \sin\phi$ ($a_\pm = \pm\pi$) respectively. The function g is assumed to be an odd, continuously differentiable function and

$$<\ g(\phi)\ >= \frac{1}{|\Omega|}\ \int_\Omega g[\phi(x)]\ dx, \tag{2}$$

where $|\Omega|$ is the size of the domain Ω. Note that linear global coupling is obtained when $g(\phi) = \phi$. We consider Neumann boundary conditions.

Eq (1) with $\gamma = 0$ has been extensively studied [1] (see also references therein). It has been used to model the propagation of crystal deffects, propagation of domain walls in ferromagnetic and ferroelectric materials, propagation of splay waves on a biological (lipid) membrane, self induced transparency of short optical pulses [1] (and references therein) and solid-liquid phase transitions in systems with memory [2, 3].

Of particular interest has been the study of evolution of fronts or interfaces for the Klein-Gordon equation [1, 4–6] and oscillations of eccentric pulsons in the sine-Gordon equation [1, 7]. Probably the most important application of the sine-Gordon equation is as a model

for the propagation of transverse electromagnetic (TEM) waves in a superconducting strip line transmission system [1]. In this model the order parameter ϕ represents the change in phase of the superconducting wave function across a barrier, and its time derivative is proportional to the voltage. In this case $1/D$ is equal to the product of the inductance per unit length of the strip line and the capacitance per unit length, and $\alpha = 2\,e\,I_0/(\sqrt{D}\,\hbar)$ where e is the electronic charge, $\hbar$ is Planck's constant divided by π and $I_0 \sin(\phi)$ is the Josephson tunneling of superconducting electrons through the insulating barrier.

In the one-dimensional case, when $\eta = 0$ (no dissipation), $h = 0$, $\alpha = 1$ and $\gamma = 0$ (no global coupling), equation (1) has a kink (soliton) traveling with a velocity c that can be calculated from the parameters of the model. A kink is a solution that connects the two local minima of the double well potential (phases of the system); i.e., a monotonic level change of magnitude $a_+ - a_-$ as $x - c\,t$ moves across the interval $(-\infty, \infty)$ [1, 8]. In the case of the prototype Klein Gordon and sine-Gordon equations these solutions for $D = 1$ are given by

$$\phi(x,t) = 4\tan^{-1}\left(e^{\frac{x-c\,t}{\sqrt{1-c^2}}}\right) \qquad \text{and} \qquad \phi(x,t) = \tanh\left(\frac{x-c\,t}{\sqrt{1-c^2}}\right)$$

respectively.

The one-dimensional case corresponds to a situation in which one of the transverse directions is smaller than a characteristic length.

When both transverse directions are larger than this characteristic length, Josephson junctions are essentially two dimensional [4, 6, 7, 9–11]. It is possible to find two-dimensional solutions for eq. (1) that locally look like kinks in a direction normal to a curve separating the two phases [1, 7, 12]. We call these solutions quasi two-dimensional (Q2D) kinks. In particular, if the curve is a closed circle, then this Q2D kink soliton represents a fluxon loop [1, 7, 12, 13]. This circular fluxon loop becomes a metastable pulson, since its radius will increase until it reaches a maximum. Then the circular fluxon collapses, shrinking to a minimum size before being reflected again.

If $h \neq 0$ and $\gamma = 0$ (no global coupling) in eq. (1), only one-phase solutions are stable; i.e., initially heterogeneous front or front-like solutions (Q2D kinks in the two dimensional case) evolve towards homogeneity. The discrete and semidiscrete versions of eq. (1) (with $\gamma = 0$

and $h \neq 0$) display a richer behavior. There one can find localized solutions in which one phase is stabilized inside the other [13–15] (and see references therein).

In this manuscript we study the role of global coupling in creating localized solutions for (1); i.e., in stabilizing one phase inside the other. The effect of global coupling or interactions has been studied in many chemical [16–30], physical [31–37] and biological [38–40] systems. In particular in [34] (see also [37]) the dynamics of an overdamped, discrete, globally coupled Josephson junction array with no local coupling is studied. In general, the global coupling term has been taken as the integral over the whole domain (or the sum over all the elements of the discret system) either of the order parameter or of other variables (usually concentration) according to the physical situation. Here, we follow [34] and take the global coupling over the order parameter ϕ.

In order to put equation (1) into dimensionless form we call L the size of Ω in the one-dimensional case, the size of the largest side of Ω in the rectangular case, or the diameter of the minimal circle that surrounds Ω in other two-dimensional domains. Next we define the following dimensionless variables and parameters

$$\hat{x} = \frac{x}{L}, \qquad \hat{y} = \frac{y}{L}, \qquad \hat{t} = \frac{\sqrt{D}\, t}{L} \tag{3}$$

and

$$\epsilon = \sqrt{\frac{D}{\alpha}}\, \frac{1}{L} \qquad \hat{\eta} = \frac{\eta\ L}{\sqrt{D}} \qquad \hat{\gamma} = \frac{\gamma\ L}{\sqrt{\alpha D}}, \qquad \hat{h} = \frac{h}{\epsilon}. \tag{4}$$

Substituting (3) and (4) into (1), dropping the ''hat" sign from the variables and parameters and rearranging terms we get

$$\epsilon^2\ \phi_{tt} + \epsilon^2\ \eta\ \phi_t = \epsilon^2\ \Delta\phi + f(\phi) + \epsilon\ h + \epsilon\ \gamma\ < g(\phi) > . \tag{5}$$

We will consider the case $0 < \epsilon \ll 1$.

When $\gamma = 0$ (no global coupling), equation (5) posseses a front (travelling kink) solution in which the transition between the two minima of $f(\phi)$ takes place in a region of order of magnitude $\epsilon \ll 1$; i.e., the kinks have rapid spatial variation between the two ground states (phases) [6]. The point on the line (for $n = 1$) or the set of points in the plane (for $n = 2$)

for which the order parameter ϕ vanishes is called the interface of the front. Points in Ω that are at least $\mathcal{O}(\epsilon)$ away from the interface can be approximated by $\phi(z) = a_+ + \mathcal{O}(\epsilon)$ or $\phi(z) = a_- + \mathcal{O}(\epsilon)$ according to whether they are on one or the other side of the interface. One can study the motion of the front by studying the motion of its interface. We use the functions $s = s(x,t)$ and $\rho = \rho(\theta,t)$ to describe the interface in cartesian and polar coordinates respectively. Note that $s = s(t)$ and $\rho = \rho(t)$ describe one-dimensional and a circular two-dimensional interfaces respectively.

For eq. (5) with $\gamma = 0$ (no global coupling) fronts move according to an extended version of the Born-Infeld equation [5, 6]

$$(1 - s_t^2)\ s_{xx} + 2\ s_x\ s_t\ s_{xt}\ - (1 + s_x^2)\ s_{tt} - \eta\ s_t\ (1 + s_x^2 - s_t^2) - h_e\ (1 + s_x^2 - s_t^2)^{\frac{3}{2}} = 0, \quad (6)$$

where h_e, proportional to h, will be defined later. Planar fronts moving according to (6) with $\eta = h_e = 0$ (no dissipation and both phases with equal potential) move with a constant velocity equal to their initial velocity. For other values of η or h_e, fronts move with a velocity that asymptotically approaches $-h_e/(\eta^2 + h_e^2)^{\frac{1}{2}}$ as long as the initial velocity is bounded from above by 1 in absolute value [6]. Linear perturbations to these planar fronts decay, in either a monotonic or an oscillatory way, to zero as $t \to \infty$ [6]. Circular interfaces moving according to (6) with $h > 0$ shrink to a point in finite time [5, 6]. If $h < 0$, there exists a value h_0 such that circles shrink to points for values of $h > h_0$, and if $h < h_0$ fronts grow unboundedly. Neu [5] showed that for $\eta = h = 0$, closed kinks can be stabilized against collapse by the appearance of short wavelength, small amplitude waves. For the more general case, perturbations to a circle may decay or not. If they do, the perturbed circles shrink to a point in finite time. Note that Equation (6) expressed in terms of its kinematic and geometric properties reads [6]

$$\frac{dv}{dt} + \eta\ v\ (1 - v^2) - \kappa\ (1 - v^2) + h_e\ (1 - v^2)^{\frac{3}{2}} = 0, \quad (7)$$

where κ is the curvature of the front and dv/dt is the "Lagrangian" time derivative of v which is calculated along the trajectory of the interfacial point moving with the normal velocity v [6].

The outline of the paper is as follows. In Section II we present an equation (leading order

term approximation) describing the evolution of fronts for (5) that includes the effect of global feedback ($\gamma \geq 0$) on the dynamics, and we briefly describe its derivation from (5). In Section III we study the evolution of one-dimensional fronts. We find that, due to the effect of global coupling, one phase can be stabilized inside the other, and we present an expression for the fraction of the one-dimensional domain Ω in each phase as a function of γ, L and h. The dynamics of two-dimensional fronts with radial symmetry is analyzed in Section IV. As in the one-dimensional case, we find that, due to the effect of global coupling and depending on the values of the parameters γ, h, η and L, one phase can be stabilized inside the other. In Section V we show that localized circular fronts are linearly stable. Our conclusions appear in Section VI.

II. FRONT DYNAMICS: THE EQUATION OF MOTION

For (5) the motion of a front is governed by the Born-Infeld equation with global coupling, an equation that generalizes (6):

$$(1-s_t^2)\ s_{xx} + 2\ s_x\ s_t\ s_{xt}\ - (1+s_x^2)\ s_{tt} - \eta\ s_t\ (1+s_x^2-s_t^2) -$$

$$-h_e\ (1+s_x^2-s_t^2)^{\frac{3}{2}} - \gamma_0\ (1+s_x^2-s_t^2)^{\frac{3}{2}}\ < g(\psi) >= 0 \tag{8}$$

where $y = s(x,t)$ is the Cartesian description of the interface and h_e and γ_0 are proportional to h and γ, respectively as will be explained later. The function ψ (independent of ϵ) satisfies $\phi = \psi + \mathcal{O}(\epsilon)$ in a small enough neighborhood of the interface.

For the study of closed convex fronts we will use the polar coordinate version of (8) which is given by

$$(1-\rho_t^2)\ \rho_{\theta\theta} + 2\ \rho_\theta\ \rho_t\ \rho_{\theta t} - (\rho^2+\rho_\theta^2)\rho_{tt} - \eta\ \rho_t\ [\rho^2\ (1-\rho_t^2)+\rho_\theta^2] -$$

$$\rho\ (1-\rho_t^2) - 2\ \frac{\rho_\theta^2}{\rho} - \frac{h_e}{\rho}\ [\rho^2\ (1-\rho_t^2)+\rho_\theta^2]^{\frac{3}{2}} -$$

$$\frac{\gamma_0}{\rho}\ [\rho^2\ (1-\rho_t^2)+\rho_\theta^2]^{\frac{3}{2}}\ < g(\psi) > = 0 \tag{9}$$

where $\rho = \rho(\theta, t)$ represents the interface and h_e and γ_0 are defined below as in the Cartesian case.

Equation (8) is obtained by carrying out a non-rigorous but self-consistent singular perturbation analysis for $\epsilon \ll 1$, treating the interfaces as a moving internal layer of width $O(\epsilon)$. We focus on the dynamics of the fully developed layer, and not on the process by which it is generated. The derivation, which we sketch below, is similar to that used in [6] for the study of the evolution of kinks in the nonlinear wave equation (5) with $\gamma = 0$. The basic assumptions made are:

- For small $\epsilon \geq 0$ and all $t \in [0, T]$, the domain Ω can be divided into two open regions $\Omega_+(t;\epsilon)$ and $\Omega_-(t,\epsilon)$ by a curve $\Gamma(t;\epsilon)$, which does not intersect $\partial\Omega$. This interface, defined by $\Gamma(t;\epsilon) := \{x \in \Omega : \phi(x,t;\epsilon) = 0\}$, is assumed to be smooth, which implies that its curvature and its velocity are bounded independently of ϵ.

- There exists a solution $\phi(x,t;\epsilon)$ of (5), defined for small ϵ, for all $x \in \Omega$ and for all $t \in [0,T]$ with an internal layer. As $\epsilon \to 0$ this solution is assumed to vary continuously through the interface, taking the value 1 when $x \in \Omega_+(t;\epsilon)$, -1 when $x \in \Omega_-(t,\epsilon)$, and varying rapidly but smoothly through the interface.

- The curvature of the front is small compared to its width.

By setting $\epsilon = 0$, one obtains that the zeroth order approximation of (5) is $\phi_0 = a_\pm$ (the two stable solutions of $f(\phi) = 0$) for points on Ω in $\Omega_\pm$. For points on Ω in a $\mathcal{O}(\epsilon)$ neighborhood of $\Gamma(t)$, we define near the interface a new variable $z = (y - s(x,t))/\epsilon$, which is $\mathcal{O}(1)$ as $\epsilon \to \infty$, and then express equation (5) in terms of this new variable. After equating the coefficients of corresponding powers of ϵ, we obtain two equations describing the evolution of the first and second order approximations. A rescaling $\xi = z\,/(1 + s_x^2 - s_t^2)$ reduces the first equation to $\Psi_{\xi\xi} + f(\Psi) = 0$, which has to satisfy $\Psi(0) = 0$ and $\Psi(\pm\infty) = \pm a$, giving a kink solution (see Section I). Here Ψ represents the leading order term of the order parameter ϕ as a function of ξ. The second equation, describing the evolution of the first order approximation to ϕ (in a neighborhood of the interface), is a linear non-homogeneous second order ODE (in ξ). Its homogeneous part has $\Psi'(\xi)$ has a solution. The solvability condition (Fredholm alternative) requires that the the integral of the non-homogeneous part multiplied by $\Psi'(\xi)$ over the real

numbers (or equivalently over the $\mathcal{O}(\epsilon)$ width of the interface) must be zero. Equation (8) results from applying the solvability conditions after rearranging terms and defining

$$h_e := \frac{h\ [\Psi(+\infty) - \Psi(-\infty)]}{\int_{-\infty}^{\infty}(\Psi')^2 d\xi} = \frac{2\,a\,h}{\int_{-\infty}^{\infty}(\Psi')^2 d\xi} \tag{10}$$

and

$$\gamma_0 = \frac{\gamma\ [\Psi(+\infty) - \Psi(-\infty)]}{\int_{-\infty}^{\infty}(\Psi')^2 d\xi} = \frac{2\,a\,\gamma}{\int_{-\infty}^{\infty}(\Psi')^2 d\xi}. \tag{11}$$

We refer to [6] for details in the procedure. Eq. (9) can be obtained from eq. (5), expressed in polar coordinates, following the same procedure as for eq. (8).

In this way the first order approximation of ϕ is given by

$$\phi = \begin{cases} a_+ & \mathbf{x} \in \Omega_+, \\ a_- & \mathbf{x} \in \Omega_-, \\ \Psi(\mathbf{x}/\epsilon) & \mathbf{x} \in \Gamma, \end{cases} \tag{12}$$

For an odd function $g(\phi)$,

$$< g(\psi) > \sim \frac{1}{|\Omega|} \int_{\Omega/\Gamma} g[\phi^0(x)]\ dx =$$

$$\frac{1}{|\Omega|} \left[\int_{\Omega_+} g[\psi(\infty)]\ dx + \int_{\Omega_-} g[\psi(-\infty)]\ dx \right]. \tag{13}$$

It can be easily seen that

$$< g(\psi) > \sim\ g(1)\ \frac{|\Omega| - 2\ |\Omega_-|}{|\Omega|},$$

since $|\Omega| \sim |\Omega_+| + |\Omega_-|$. Calling

$$\gamma_e = \frac{\gamma_0\, g(1)}{|\Omega|}, \tag{14}$$

equations (8) and (9) become

$$(1 - s_t^2)\ s_{xx} + 2\ s_x\ s_t\ s_{xt}\ - (1 + s_x^2)\ s_{tt} - \eta\ s_t\ (1 + s_x^2 - s_t^2) -$$

$$-[\ h_e\ +\ \gamma_e\ (\ |\Omega| - 2\ |\Omega_-|\ )\ ]\ (1 + s_x^2 - s_t^2)^{\frac{3}{2}}\ = 0, \tag{15}$$

and

$$(1-\rho_t^2)\ \rho_{\theta\theta} + 2\ \rho_\theta\ \rho_t\ \rho_{\theta t} - (\rho^2+\rho_\theta^2)\rho_{tt} - \eta\ \rho_t\ [\rho^2\ (1-\rho_t^2) + \rho_\theta^2] -$$

$$\rho\ (1-\rho_t^2) - 2\ \frac{\rho_\theta^2}{\rho} - \frac{h_e + \gamma_e\ (\ |\Omega| - 2\ |\Omega_-|\ )}{\rho}\ [\rho^2\ (1-\rho_t^2) + \rho_\theta^2]^{\frac{3}{2}} = 0. \tag{16}$$

Note that for $f(\phi) = \frac{\phi - \phi^3}{2}$ (the Ginzburg-Landau case), $\Psi(\xi) = \tanh\frac{\xi}{2}$, $h_e := 3\ h$ and $\gamma_e = 3\,\gamma$, whereas for $f(\phi) = \sin\phi$, $\Psi(\xi) = 4\ \tan^{-1} e^{\xi} - \pi$, $h_e := \frac{\pi}{4}\ h$ and $\gamma_e := \frac{\pi}{4}\ \gamma$.

III. DYNAMICS OF ONE-DIMENSIONAL FRONTS

The evolution of one-dimensional fronts in a domain $\Omega = [0,1]$ is given by

$$s_{tt} + \eta\ s_t\ (1-s_t^2) + (\ h_e + \gamma_e\ )\ (1-s_t^2)^{\frac{3}{2}} - 2\ \gamma_e\ s\ (1-s_t^2)^{\frac{3}{2}} = 0, \tag{17}$$

which has been obtained from (15) by taking $|\Omega| = 1$ and $|\Omega_-| = s$. Calling $v = s_t$, equation (17) becomes

$$\begin{cases} s_t = v, \\ v_t = -\eta\ v\ (1-v^2) - (\ h_e + \gamma_e\ )\ (1-v^2)^{\frac{3}{2}} + 2\ \gamma_e\ s\ (1-v^2)^{\frac{3}{2}}. \end{cases} \tag{18}$$

For every h_e and every γ_e, system (18) has one equilibrium point

$$(\bar{s}, \bar{v}) = \left(\frac{h_e\ + \gamma_e}{2\ \gamma_e}, 0 \right). \tag{19}$$

The trace and determinant of the matrix of the coefficients of the linearization of system (18) are $-\eta$ and $-2\ \gamma_e$ respectively. Thus, $(\bar{s}, \bar{v})$ is stable for $\gamma_e < 0$ and $\eta > 0$, a center for $\gamma_e < 0$ and $\eta = 0$, and a saddle point for $\gamma_e > 0$. That means that in order to get coexistence of two phases the global feedback must be inhibitory ($\gamma < 0$). Note that when $h_e = 0$ (no difference of potential between the two phases), $\bar{s} = 1/2$; i.e., the two phases will coexist, with half the domain in each phase. When $h_e > 0$ (< 0), $\bar{s} < 1/2$ ($> 1/2$). From the fact that $0 \le \bar{s} \le 1$ we get the following constraint for the existence of a stable front:

$$\left| \frac{h_e}{\gamma_e} \right| \le 1. \tag{20}$$

For $\eta = 0$ (no damping) the solution of (18), for an arbitrary constant c, is

$$v^2 = 1 - [\ \gamma_e\ s^2 - (\ h_e + \gamma_e)\ s + c\ ]^{-2}. \tag{21}$$

In Fig. 1 we illustrate the evolution of one-dimensional fronts for different values of γ_e, h_e and η. (All numerical simulations presented in this paper have been performed using a Runge-Kutta method of order four [41].) Initially $s_t = 0$ in all cases. As stated in the introduction, in the absence of global coupling ($\gamma_e = 0$) fronts move with a velocity that asymptotically approaches $-h_e/(\eta^2 + h_e^2)^{\frac{1}{2}}$ [6], and no localized structures exist. We show this in Fig. 1-a for various values of h_e and $\eta = 0$ (no dissipation). We ended the simulations at $s = 1$, since this is the upper bound of the dimensionless interval on which the dynamics is defined.

Fronts moving under inhibitory global feedback ($\gamma_e < 0$) with dissipation ($\eta > 0$) evolve to a localized solution where the position of the front is given by (19), and they do so in a damped oscillatory way as we illustrate in Fig. 1-b. The larger η the smaller the amplitude of the oscillations. When $\eta = 0$ (no dissipation) fronts oscillate with no damping. In this case the two phases coexist but there is no stabilization of one phase within the other. In Fig. 1-c we show that the amplitude of these oscillations increases as h_e decreases. Note that in all cases illustrated here, oscillatory fronts do not move below their initial position. Note as well that in order to constrain oscillatory fronts to the dimensionless interval $[0, 1]$ one may need to impose additional constraints on the values of the parameters (h_e and γ_e) or, alternatively, end the simulations when the front $s(t)$ reaches either 0 or 1.

IV. DYNAMICS OF TWO-DIMENSIONAL FRONTS WITH RADIAL SYMMETRY

The evolution of two-dimensional fronts with radial symmetry in a square domain is given by

$$\rho_{tt} + (\eta\ \rho_t\ + \frac{1}{\rho})\ (1 - \rho_t^2) + [\ h_e + \gamma_e - 2\ \gamma_e\ \pi\ \rho^2\ ]\ (1 - \rho_t^2)^{\frac{3}{2}} = 0, \tag{22}$$

which has been obtained from (16) by taking Ω to be a square of side 1 and $|\Omega_-| = \pi\ \rho^2$. Writing v for ρ_t, equation (22) becomes

$$\begin{cases} \rho_t = v, \\ v_t = -[\ \eta\ v + 1/\rho\ ]\ (1-v^2) - (\ h_e + \gamma_e\ )\ (1-v^2)^{\frac{3}{2}} + 2\ \gamma_e\ \pi\ \rho^2\ (1-v^2)^{\frac{3}{2}} = 0. \end{cases} \tag{23}$$

The equilibrium solutions of (23) are given by $\bar{v} = 0$ and $\bar{\rho}$ a solution of

$$2\ \gamma_e\ \pi\ \bar{\rho}^3 - (\ h_e + \gamma_e\ )\ \bar{\rho} - 1 = 0. \tag{24}$$

Note that the steady state solutions of (24); i.e., the radii ρ_{ss} of the equilibrium circular fronts, are independent of η.

The trace and determinant of the matrix of the coefficients of the linearization of system (23) are $-\eta$ and $-(1/\bar{\rho}^2 + 4\ \gamma_e\ \pi\ \bar{\rho})$ respectively. Thus solutions of (24) are stable if $\eta > 0$ and

$$1 + 4\ \gamma_e\ \pi\ \bar{\rho}^3 < 0, \tag{25}$$

and solutions of (24) are saddle points if

$$1 + 4\ \gamma_e\ \pi\ \bar{\rho}^3 > 0. \tag{26}$$

In Fig. 2 we show solutions to (24) as a function of γ_e for various values of h_e. As in the one-dimensional case, in order to have coexistence of the two phases in equilibrium the global feedback parameter must be negative. In Fig. 2 we can also see that in all cases in which we observe coexistence of two phases in equilibrium, coexistence depends on the initial radius of the front: Circular fronts whose radii are below a threshold given by the dashed curves shrink to a point in finite time. In all cases there is a value of $\gamma_e < 0$ below which steady circular fronts can be obtained and above which no localized solutions are possible. This value increases as h_e decreases. This is a fundamental difference between the one-dimensional case and the two-dimensional case with radial symmetry. In the one-dimensional case, motion of fronts depends only on h_e and γ_e, while in the two-dimensional case the curvature plays an important role, requiring values of $\gamma_e < 0$ in order to overcome the shrinking effect exerted by the front curvature (the tendency of one phase to grow at the expense of the other due to curvature effects). We can also see that the steady state radii depend on the value of γ_e. In the three panels of Fig. 2 we see that as h_e decreases, even for

small absolute values of the global feedback parameter γ_e we get two coexisting phases. The values of the steady state radii are almost constant when the inhibitory coupling is strong, but increase rapidly for small negative values of γ_e.

In Fig. 3 we illustrate the evolution of circular fronts for various values of η, h_e and γ_e. Fig. 3-a corresponds to the system with no global feedback and is presented for comparison. (The simulations for the growing fronts were ended at $s = 1.1$, but the front grows unboundedly.) In Fig. 3-b we illustrate the non-damped case ($\eta = 0$). In this case circular fronts oscillate with an amplitude and frequency that both depend on and decrease with the absolute value of γ_e. In Fig. 3-c we demonstrate that with positive η these oscillations are damped and converge to a steady (and stable) circular front.

V. DYNAMICS OF TWO-DIMENSIONAL FRONTS WITHOUT RADIAL SYMMETRY: STABILITY OF CIRCULAR FRONTS

In order to investigate the stability of steady circular fronts satisfying (25) we expand ρ in an asymptotic series in ϵ, assuming that ρ depends weakly on θ ($\rho_\theta \sim 0$):

$$\rho(t,\theta) = R_0(t) + R_1(t,\theta). \tag{27}$$

Substituting (27) into (16), and we get the leading order term and first order correction respectively:

$$R_{0,tt} + (\eta\ R_{0,t}\ + \frac{1}{R_0})\ (1 - R_{0,t}^2) + [\ h_e + \gamma_e\ - 2\ \gamma_e\ \pi\ R_0^2\ ]\ (1 - R_{0,t}^2)^{\frac{3}{2}} = 0, \tag{28}$$

and

$$R_{1,tt} = (R_{1,\theta\theta} - R_1)\ \frac{1 - R_{0,t}^2}{R_0^2} - \eta\ R_{1,t}\ (1 - R_{0,t}^2) + 2\ \frac{R_1}{R_0^2}\,(1 - R_{0,t}^2) +$$

$$+2\ \frac{R_0 + \eta\ R_0^2\ R_{0,t}}{R_0^2}\ R_{0,t}\,R_{1,t}\ + 3\ [\,h_e + \gamma_e\ (1 - 2\ \pi\ R_0^2)\,]\ R_{0,t}\ R_{1,t}\ (1 - R_{0,t}^2)^{1/2} +$$

$$+2\ \gamma_e\ R_0\ (1 - R_{0,t}^2)^{3/2} \int_0^{2\pi} R_1(t,\theta)d\theta. \tag{29}$$

Equation (28) is the same as (22), which we have already analyzed. When R_0 reaches its stable steady state, $R_{0,t} = 0$ and

$$1 + 4\ \gamma_e\ \pi\ R_0^3 < 0 \tag{30}$$

Thus, eq. (29) reduces to

$$R_{1,tt} + \eta\ R_{1,t} = \frac{R_{1,\theta\theta} + R_1}{R_0^2} + 2\ \gamma_e\ R_0\ \int_0^{2\pi} R_1(t,\theta) d\theta. \tag{31}$$

Eq. (31) is a linear integro-PDE that can be solved by expanding R_1 in a Fourier series

$$R_1(t,\theta) = \frac{A_0(t)}{2} + \sum_{n=0}^{\infty} [\ A_n(t)\ \cos n\,\theta + B_n(t)\ \sin n\,\theta\ ].$$

where the Fourier coefficients must satisfy

$$\begin{cases} A_0'' + \eta\ A_0' = A_0\ (-1 + 4\pi\gamma_e R_0^3)/R_0^2, \\ A_n'' + \eta\ A_n' = -A_n\ (1 - n^2)/R_0^2, \\ B_n'' + \eta\ B_n' = -B_n\ (1 - n^2)/R_0^2, \end{cases} \tag{32}$$

for $n = 1, \ldots$. From (30) we can easily see that $A_0(t) \to 0$. It is also clear that $A_n(t) \to 0$ and $B_n(t) \to 0$ for $n \geq 2$, $A_1(t) \to const$ and $B_1(t) \to const$; i.e., the mode $n = 1$ is not asymptotically stable but rather neutrally stable. Thus, circular fronts described by (22) are stable to small perturbations.

VI. DISCUSSION

In this manuscript we have derived an equation (8) governing the evolution of a fully developed front in a singularly perturbed nonlinear wave equation with global inhibitory feedback (5). This equation generalizes the damped version of the Born-Infeld equation (6) to include global feedback effects on the motion of fronts. The motion of interfaces according to (8) is qualitatively different from and much richer than that of its counterpart with no global coupling ($\gamma = 0$). This difference arises primarily from the fact that the presence of inhibitory global feedback allows the existence of localized solutions (or fronts) in which one phase is stabilized inside the other. In the absence of dissipation ($\eta = 0$), fronts are oscillatory. When dissipation effects are present ($\eta > 0$), the oscillations decay, spirally or not, depending on the value of γ_e. The final result is the stabilization of a domain of one phase inside the other phase. In the two-dimensional case the inhibitory feedback necessary to produce

a localized solution has to be strong enough to overcome the shrinking effect exerted by curvature.

The evolution of two-dimensional non-circular fronts calls for further research. In this paper we addressed the case of perturbed circular fronts, showing that these perturbations decay; i.e., localized solutions are possible for these cases. We hope to address more general cases in a forthcoming paper.

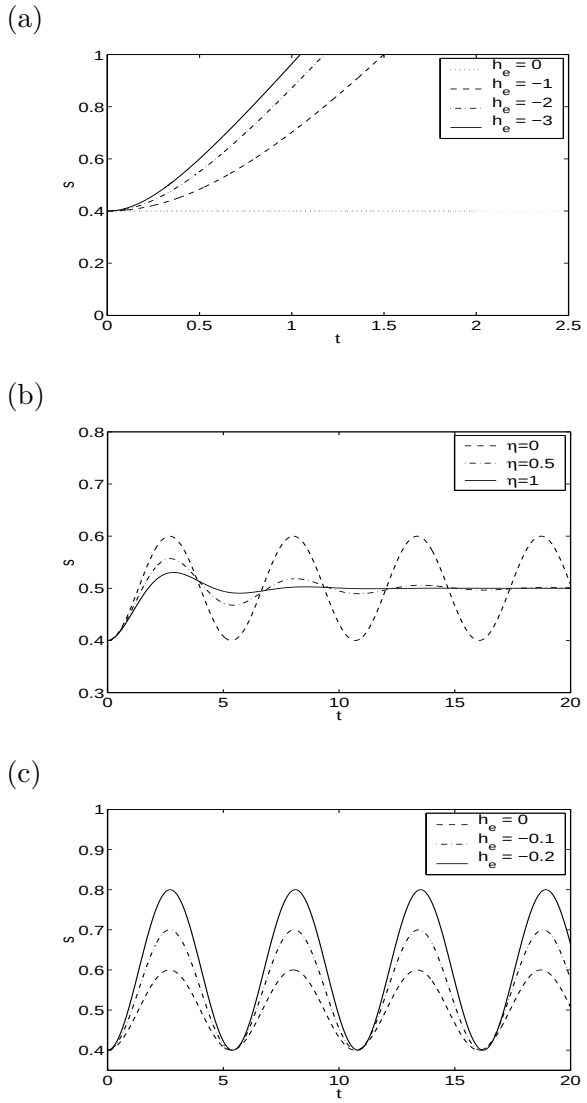

FIG. 1: Evolution of one-dimensional fronts for various values of η, h_e and γ_e. (a) $\eta = 0$ and $\gamma_e = 0$. (b) $h_e = 0$ and $\gamma_e = -1$. (c) $\eta = 0$ and $\gamma_e = -1$.

Acknowledgments

We thank Nancy Kopell, Igor Mitkov and Steve Epstein. This work was partially supported by the Fischbach Fellowship (HGR), NSF grant DMS-0211505 (HGR), NSF Grant CHE-0306262 (AMZ) and the Petroleum Research Fund of the American Chemical Society (IRE).

---

[1] A. Scott, *Nonlinear Science* (Oxford University Press, 1999).

[2] H. G. Rotstein, S. Brandon, A. Novick-Cohen, and A. A. Nepomnyashchy, SIAM J. Appl. Math. **62**, 264 (2001).

[3] H. G. Rotstein, A. Nepomnyashchy, and A. Novick-Cohen, J. Crystal Growth **198-199**, 1262 (1999).

[4] B. A. Malomed, Physica D **52**, 157 (1991).

[5] J. C. Neu, Physica D **43**, 421 (1990).

[6] H. G. Rotstein and A. A. Nepomnyashchy, Physica D **136**, 245 (2000).

[7] P. L. Christiansen, N. Gronbech-Jensen, P. S. Lomdahl, and B. A. Malomed, Physica Scripta **55**, 131 (1997).

[8] D. G. Aronson and H. F. Weinberger, Lecture Notes in Mathematics **446**, 5 (1975).

[9] J. G. Caputo, N. Flytzanis, Y. Gaididei, and M. Vavalis, Phys. Rev. E **54**, 2092 (1996).

[10] J. G. Caputo, N. Flytzanis, and M. Vavalis, Int. J. Mod. Phys. C **6**, 241 (1995).

[11] J. G. Caputo, N. Flytzanis, and M. Vavalis, Int. J. Mod. Phys. C **7**, 191 (1996).

[12] H. G. Rotstein, A. M. Zhabotinsky, and I. R. Epstein, Chaos **11**, 833 (2001).

[13] S. Flach and K. Kladko, Phys. Rev. E **54**, 2912 (1996).

[14] S. Flach and C. R. Willis, Phys. Rep. **295**, 181 (1998).

[15] H. G. Rotstein, I. Mitkov, A. M. Zhabotinsky, and I. R. Epstein, Phys. Rev. E **63**, 066613 (2001).

[16] V. K. Vanag, L. Yang, M. Dolnik, A. M. Zhabotinsky, and I. R. Epstein, Nature **406**, 389 (2000).

[17] V. K. Vanag, A. M. Zhabotinksy, and I. R. Epstein, J. Phys. Chem. **104A**, 11566 (2000).

[18] L. Yang, M. Dolnik, A. M. Zhabotinsky, and I. R. Epstein, Phys. Rev. E **62**, 6414 (2000).

[19] S. Kawaguchi and M. Mimura, SIAM J. Appl. Math. **59**, 920 (1999).

[20] F. Mertens, R. Imbihl, and A. Mikhailov, J. Chem. Phys. **99**, 8688 (1993).

[21] L. M. Pismen, J. Chem. Phys. **101**, 3135 (1994).

[22] M. Sheintuch and O. Nekhamkina, in Pattern Formation in Continuous and Coupled Systems (IMA Volumes in Mathematics and its applications), edited by M. Golubitsky, D. Luss and S. H. Strogatz (Springer-Verlag, New York) **115**, 265 (1999).

[23] M. Kim, M. Bertram, M. Pollmann, A. von Oertzen, A. S. Mikhailov, H. H. Rotermund, and G. Ertl, Science **292**, 1357 (2001).

[24] U. Middya, D. Luss, and M. Sheintuch, J. Chem. Phys. **10**, 3568 (1994).

[25] U. Middya, D. Luss, and M. Sheintuch, J. Chem. Phys. **101**, 4688 (1994).

[26] U. Middya, M. D. Graham, L. D., and M. Sheintuch, J. Chem. Phys. **98**, 2823 (1993).

[27] I. Savin, O. Nekhamkina, and M. Sheintuch, J. Chem. Phys. **115**, 7678 (2001).

[28] M. Sheintuch and O. Nekhamkina, J. Chem. Phys. **107**, 8165 (1997).

[29] U. Middya and D. Luss, J. Chem. Phys. **100**, 6386 (1994).

[30] U. Middya and D. Luss, J. Chem. Phys. **102**, 5029 (1995).

[31] H. Riecke, in Pattern Formation in Continuous and Coupled Systems (IMA Volumes in Mathematics and its Applications), edited by M. Golubitsky, D. Luss and S. H. Strogatz (Springer-Verlag) **115**, 215 (1999).

[32] S. H. Strogatz, R. E. Mirollo, and P. C. Matthews, Phys. Rev. Lett. **68**, 2730 (1992).

[33] S. H. Strogatz and R. E. Mirollo, Phys. Rev. E **47**, 220 (1993).

[34] K. Y. Tsang, R. E. Mirollo, S. H. Strogatz, and K. Wiesenfeld, Physica D **48**, 102 (1991).

[35] D. Golomb, D. Hansel, B. Shraiman, and H. Sompolinksy, Phys. Rev. A **45**, 3516 (1992).

[36] K. Wiesenfeld, in Pattern Formation in Continuous and Coupled Systems (IMA Volumes in Mathematics and its Applications), edited by M. Golubitsky, D. Luss and S. H. Strogatz (Springer-Verlag) **115** (1999).

[37] S. H. Strogatz, *Nonlinear Dynamics and Chaos* (Perseus Books, Cambridge, MA, 1994).

[38] D. Golomb and D. Rinzel, Physica D **72**, 259 (1994).

[39] D. Terman and D. L. Wang, Physica D **81**, 148 (1995).

[40] D. Golomb and D. Rinzel, Phys. Rev. E **48**, 4810 (1993).

[41] R. L. Burden and J. D. Faires, *Numerical Analysis* (PWS Publishing Company, Boston, MA, 1980).

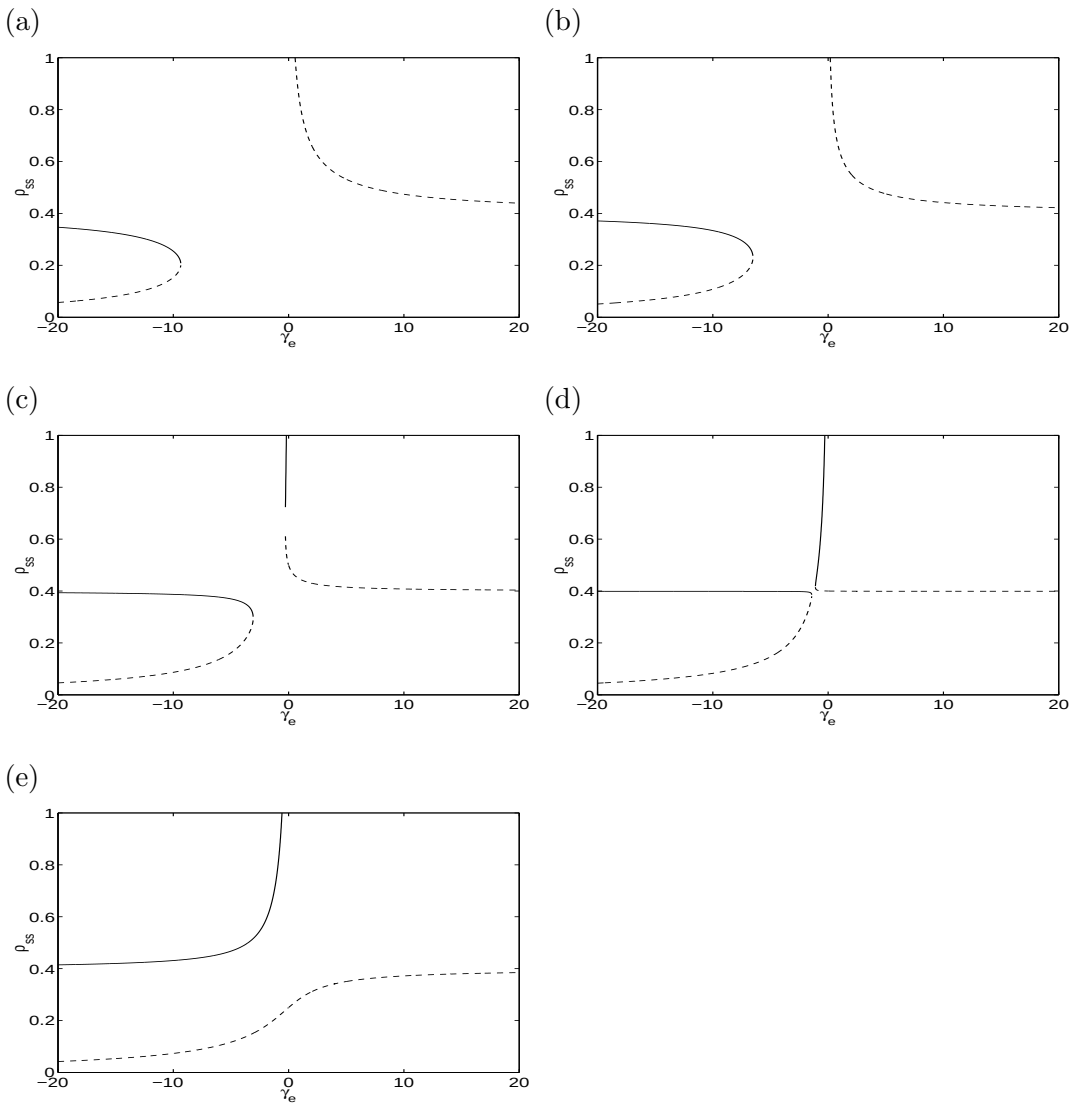

FIG. 2: Radii of the equilibrium fronts, ρ_{ss}, as a function of γ_e for a) $h_e = 2$, b) $h_e = 0$, c) $h_e = -2$, d) $h_e = -2.5$, e) $h_e = -4$. Full lines correspond to stable fronts and dashed lines correspond to unstable fronts.

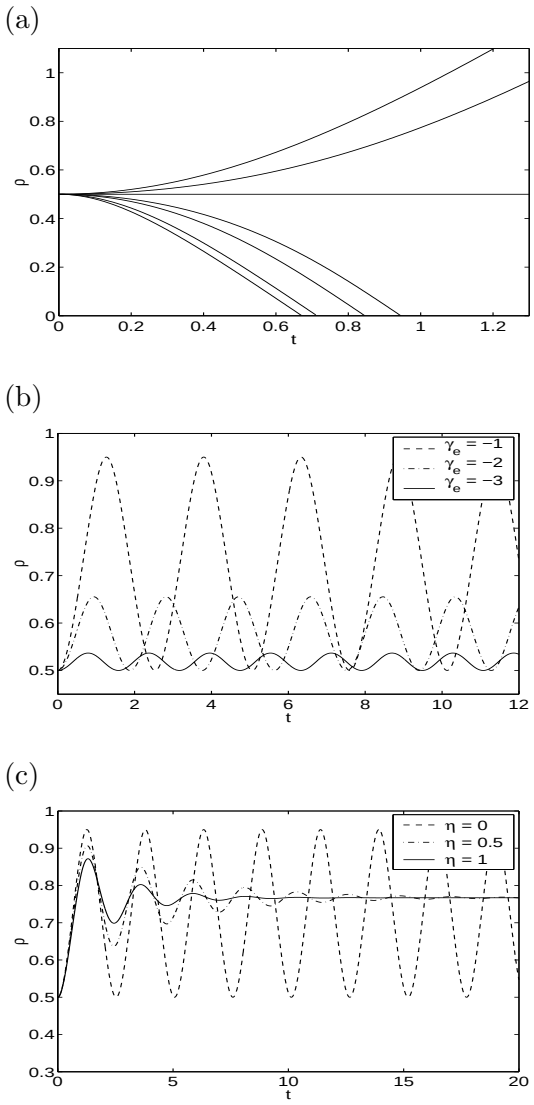

FIG. 3: Evolution of circular Q2D fronts for various values of η, h_e and γ_e. (a) $\eta = 0$ and $\gamma_e = 0$. The values of h_e (from top to bottom curves) are: $-3, -2.5, -2, -1, -0.5, 1$ and 2 respectively. For growing fronts ($h_e = -2.5, -3$ in the graph), ρ grows beyond the maximum values shown. (b) $\eta = 0$ and $h_e = 0$. (c) $\gamma_e = -1$ and $h_e = -4$.